IEEE Access
Multidisciplinary | Rapid Review | Open Access Journal

Received March 6, 2021, accepted March 31, 2021, date of publication April 8, 2021, date of current version April 16, 2021.

Digital Object Identifier 10.1109/ACCESS.2021.3071961

Monitoring Neuronal Dynamics in the Ventral Tegmental Area Using an Implantable Microimaging Device With Microdialysis System

YOSHINORI SUNAGA[1], YASUMI OHTA[2], TAKAAKI E MURAKAMI[2], YASEMIN M. AKAY[1], (Senior Member, IEEE), JUN OHTA[2], (Fellow, IEEE), AND METIN AKAY[1], (Fellow, IEEE)

[1]Biomedical Engineering Department, University of Houston, Houston, TX 77204, USA
[2]Division of Materials Science, Graduate School of Science and Technology, Nara Institute of Science and Technology, Ikoma 6300101, Japan

Corresponding author: Metin Akay (makay@uh.edu)

This work was supported in part by the University of Houston, in part by the Japan Science and Technology Agency (JST), Core Research for the Evolutionary Science and Technology (CREST), Japan, under Grant JPMJCR1651, and in part by the Japan Society for the Promotion of Science (JSPS) Grants-in-Aid for Scientific Research (KAKENHI), Japan, under Grant JP18H03780.

ABSTRACT To monitor dopamine neural activities in the ventral tegmental area (VTA) in response to nicotine, we designed a dopamine platform based on a microimaging device and a microdialysis system. We measured dopamine (DA) release in the prefrontal cortex (PFC) and the nucleus accumbens (NAc) by a micro dialysis system and monitored DA neurons activities by fluorescence imaging in the VTA using a microimaging device simultaneously. GCaMP6 transgenic mice were used in this study, and the change in the fluorescence ratio intensity associated with nicotine administration was estimated. Our results suggested that nicotine administration increased the DA neurons activity in the VTA as well as the DA release in the PFC and the NAc. The proposed platform has the potential to monitor neural activities in the deep brain regions of rodents.

INDEX TERMS Nicotine, dopamine, VTA, implantable imaging device, fluorescence imaging, GCaMP, microdialysis, PFC, NAc.

I. INTRODUCTION

Dopamine (DA) is a neurotransmitter which plays critical roles in pleasure, motivation, and learning. Excitation of DA neurons in the ventral tegmental area (VTA) leads to DA release in the nucleus accumbens (NAc), prefrontal cortex (PFC), amygdala and hippocampus [1]–[3]. Especially, DA neurons in the VTA have a strong connection to the NAc and the PFC for DA release (Fig. 1). Although this connection has been well established, quantifying the simultaneous dynamics of the DA neural network and activities within multiple regions, including regions in deep brain such as the VTA and the NAc, has been challenging. To overcome this challenge, several measurement systems have been developed including the combination of a microdialysis system and positron emission tomography (PET) technology [4]. DA release in the PFC was quantified using a microdialysis probe while brain activities by PET were monitored. This approach enabled simultaneous measurements of brain activities via imaging with biochemistry methods. However, PET technology is inadequate to monitor neural-level activity due to limitation of time and special resolution. Fluorescence imaging is one of the most promising methods to observe neural-level activity. By combining fluorescence imaging technology and optical markers such as Green fluorescence protein (GFP), targeted neural activity can be observed through fluorescence reactions. To access the deep brain area for fluorescence imaging, an optical fiber bundle or fluorescence microscope with a Gradient-Index (GRIN) lens are commonly used [5]–[9]. However, the small size of the rodent brain still poses many challenges. Therefore, new technologies utilizing optical fiber systems have been developed to observe rodent brain activity. These technologies combine high-quality images with conventional optical microscopy. However, to study larger portions of the brain, a wide-range optical fiber platform is required. The image size depends on the optical fiber diameter, which is correlated to the invasiveness. Subsequently, it is difficult to gain large

The associate editor coordinating the review of this manuscript and approving it for publication was Henry Hess.

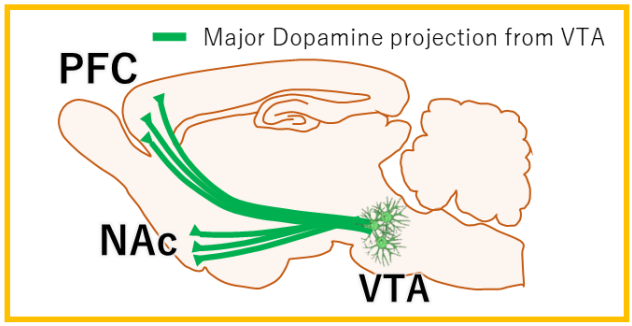

FIGURE 1. Schematic of midsagittal cross section of mouse brain. The Prefrontal Cortex (PFC) and the Nucleus Accumbens (NAc) are influenced by Dopamine (DA) neural activity in the Ventral Tegmental Area (VTA).

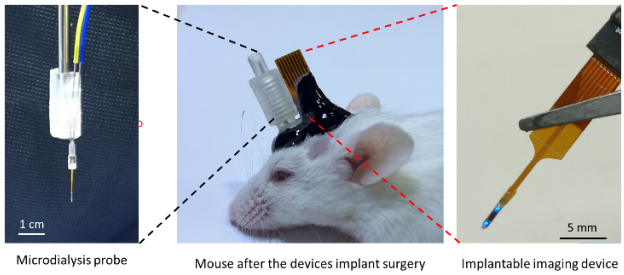

FIGURE 2. Concept of microimaging and microdialysis system. (Left) Photograph of the microdialysis probe. Scale bar is 1 cm. (Center) Photograph of a mouse after surgery to implant the probe and the imaging device. The devices were fixed using dental cement and painted black. (Right) Photograph of the implantable microimaging device. Scale bar is 5 mm.

images that cover a significant part of the brain using methods an optical fiber approach. In addition, an optical fiber is rather rigid compared to an electrical wire, and may hinder the use of it to record neural activities from freely moving animals [10]–[13].

The combination of an ultra-small fluorescence microscope and a GRIN lens with electrical cables was proposed as a method to obtain larger views with higher spatial resolution on the micrometer scale while not hinder rodent behavior [9], [14]. However, this system weighs ∼2 g, which is ∼10% the weight of an average mouse. Additionally, the typical dimensions of a probe using this technology is 8.8 mm × 15 mm × 22 mm, making it difficult to combine with microdialysis systems to monitor neural activity and simultaneous DA release. Furthermore, these methods only allow us to observe reactions along the horizontal plane.

To solve these problems, we have proposed and developed a novel microimaging [15], [16] and dialysis platform. The imaging device consists of a small Complementary Metal Oxide Semiconductor (CMOS) image sensor, micro-LEDs and a fluorescence filter on a flexible printed circuit (FPC) substrate. This small device is lightweight and can be implanted in conjunction with a micro dialysis system within the deep brain region such as the VTA of rodents with minimal invasiveness. Using this novel platform, both the DA neural activity of the VTA and the DA release in the NAc and PFC can be measured simultaneously to investigate the mechanism of the DA neural network in the brain.

In this study, we improved our previously reported implantable imaging device by using two LEDs and introducing a light-shield material. This light-shield was placed between a sensor chip and the LEDs to reduce the influence of the LED excitation light. Our new platform consists of an implantable microdialysis and fluorescence imaging system to measure brain activity related with DA network as shown in Fig. 2.

II. METHODS

A. IMPLANTABLE IMAGING DEVICE

In this study, we improved previously reported microimaging device to observe rodent brain activity under freely moving conditions using optical imaging methods, fluorescence imaging and blood flow imaging based on CMOS image sensor technology [15]–[21]. We have designed scalable image sensors which are dependent upon the measurement's targets or areas. To perform fluorescence imaging, we integrated two LEDs and an optical filter with the CMOS image sensor on a flexible printed circuit (Taiyo Industrial Co., Japan). The whole device was coated with Parylene-C to add biocompatibility and water protection. The implantable imaging device can be driven by only 6 wires and did not restrict animal behavior.

The microimaging sensors for deep brain measurements were designed using the standard CMOS process (0.35-μm, 2-poly-4 metal CMOS; TSMC, Taiwan). The pixel size is 7.5 × 7.5 μm and we used 40 × 90 pixels (0.3 × 0.675 mm) during image acquisition. In our previous *in vitro* experimental study, we determined the actual spatial resolution of the microimaging device is 22.3 ± 0.5 μm [17]. Although it may not be sufficient to observe the activities of individual neurons, this imaging sensor can provide very useful information about the dynamics of synchronizing neural activities from multiple neurons in the region of interest.

We utilized two LEDs (EPISTAR Corp., Taiwan) on upper and lower positions of the image sensor as excitation light sources. The dimensions of the LEDs are 305 × 280 μm and the central emission wavelength is 473 nm. In this study, we introduced two LEDs to provide uniform excitation light to the brain to gather higher quality images. Our preliminary data determined that the rise of the LEDs' temperature was less than 1.2°C.

We also integrated a custom flat and thinner fluorescence filter from a yellow dye (Valifast yellow 3150 (Orient Chemical, Japan)), cyclopentanone (FUJIFILM Wako Pure Chemical Corporation, Japan), and the resin (NOA63, Norland Products, USA). The custom-made filter was implemented on the image sensor surface.

In this study, we introduced a light-shield resist on side-surface of the image sensor to reduce leakage of excitation light from LEDs. A light-shield resist was consisted by mix solutions of red, blue and green resists (SR-3000L,

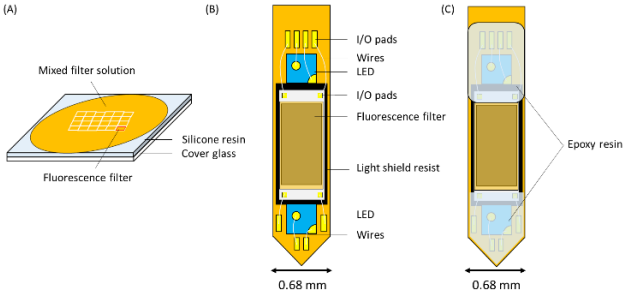

FIGURE 3. Fabrication process of a typical implantable imaging device. (A) The fluorescence filter was coated on the platform and cut to size of the image sensor. (B) The fluorescence filter was fixed onto the surface of the image sensor. The image sensor was fixed to the fluorescence filter and two LEDs on a flexible substrate (FPC). Light-shield resist was used to cover side surface of the image sensor and connected to the FPC, the image sensor and LEDs by wires. (C) The I/O pads and wires were covered by epoxy resin for protection. The whole device was coated with Parylene-C for biocompatibility.

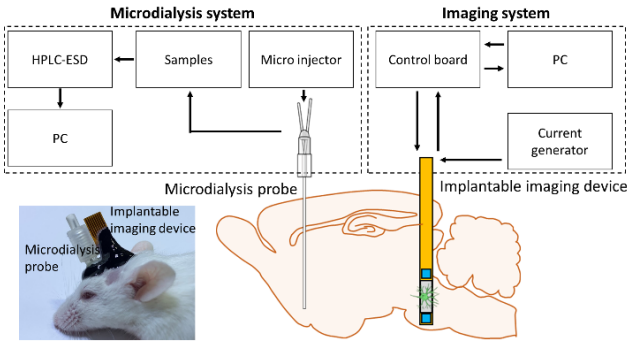

FIGURE 4. Schematic of DA network monitoring system. The microdialysis system and imaging system were driven separately. The microdialysis system was driven by a microinjector and used HPLC-ECD for measurements and analysis, and a computer controlled the HPLC-ECD. The imaging system was driven by a dedicated control board for the image sensor, a current generator for LEDs and a computer for driving the control board.

SB-3000L, SG-3000L, Fujifilm Electronic Materials CO., LTD, Japan) at a weight ratio of 1:1:1. The light-shield resist was hard-cured by heating to 120°C for 10 minutes. After the light-shield resist was hard-cured, all wires and I/O pads were covered by epoxy resin. At the end of the process, the whole device was covered with the Parylene. The thickness of the Parylene was approximately 3.1 μm, did not affect the flexibility. The fabrication of the imaging device process including light-shield resist is shown in Fig. 3(A)-(C).

B. GCaMP FLUORECENCE IMAGING

To monitor calcium signals associated with nicotine administration in DA neurons of the VTA, we used GCaMP6 transgenic mice. The implantable device was implanted in the VTA. Excitation light (473 nm) from the LEDs was used to stimulate DA neurons and GCaMP fluorescence emission was captured by a CMOS image sensor coated with a yellow fluorescence filter. This device enabled the observation of the vertical plane of the brain, which has been historically difficult to achieve with conventional methods. We obtained data from the mice brains before and after nicotine ((−)-Nicotine, Sigma-Aldrich, USA) solution administration (0.25 mg/kg) via intraperitoneal (IP) injection. Similar observations were made for the other animals in our study (n = 2 for the PFC, n = 1 for the NAc). We used the data collected prior to the nicotine administration as the control. Data was obtained using a collection rate of 10 fps from the freely moving animals. Light intensity of the LED was controlled by a current generator.

C. MICRODIALYSIS SYSTEM AND MEASAUREMENT

To measure DA release in the PFC or NAc associated with nicotine intake, we used a microdialysis system. A single microdialysis probe (EICOM, Japan) was implanted into the PFC or the NAc of the mice and connected to a microdialysis device via a micro-injection tube using Ringer's solution. The microdialysis probe was perfused at 1 μl/min and gathered 15 μl for per samples to obtain 10 μl solution for analysis. Six to eight samples were collected while the animal became stable and were used to determine baseline DA release before nicotine administration. Samples were analyzed using high performance liquid chromatography - electrochemical detection (HPLC-ECD) (EICOM) as described in Method section G.

D. DA NETWORK MONITORING SYSTEM

Compared to ultra-small fluorescent microscopy that can be mounted on a rodent head [9]–[12] and a microdialysis probe, our smaller and lighter implantable device is advantageous for experiments with multiple platforms. In this study, we combined our mountable imaging system and a traditional microdialysis system to simultaneously monitor DA network from two brain areas. We observed fluorescence activity in the VTA by our imaging system while also measuring DA release in the PFC or the NAc. The imaging system and the microdialysis system were driven separately as described in Fig. 4. Both the imaging device and the microdialysis probe were fixed together. Wires for the imaging system and tubes for the microdialysis system were only connected during experiments.

E. ANIMAL TREATMENT

All experiments were performed in accordance with the protocols approved by the Nara Institute of Science and Technology (NAIST). Adult FVB-Tg (Thy1-GCaMP6)5Shi mice (Riken BRC) (n = 3) were maintained on a 12-h light/12-h dark schedule. Access to standard food and water was *ad libitum*. Animals were mounted in a stereotaxic apparatus (Narishige, Japan) during surgery.

F. SURGERY

In this study, to monitor calcium signals in DA neurons of the VTA, we used transgenic GCaMP6 mice. All animals were anesthetized with Avertin during surgery to implant the

imaging device and the microdialysis probe. The probe and the device were implanted through a small burr hole made above the NAc (anteroposterior (AP) = 1.4 mm, mediolateral (ML) = ±0.5 mm) or PFC (AP = 1.94 mm, ML = ±0.3 mm) and VTA (AP = −3.6 mm, ML = ±0.4 mm) using a micro-drill and a manipulator. A guide cannula of the microdialysis probe was implanted in the PFC (dorsoventral (DV) = 0.25 mm from brain surface), and NAc (DV = 3.3 mm from brain surface), and the imaging device was implanted into the VTA (DV = 4.7 mm from brain surface). The guide cannula and the imaging device were sealed and closed using dental cement (Super Bond C&B, Sun Medical Co., LTD., Japan). The dental cement was painted black to eliminate the influence of light leakage from room light to the implantable imaging device.

G. HPLC ANALYSIS

To measure and analyze DA release from the PFC or the NAc, we used a HPLC-ECD. Microdialysis samples were collected every 15 minutes since at least 10 to 15 minutes are needed to get enough detectable DA releases. 10 μl from each sample were immediately injected into the HPLC-ECD to quantify DA release. After the experiments, we calculated baseline DA release by averaging the DA release amount of at least two samples gathered before nicotine administration. Then, we normalized DA release of all the samples based on the baseline.

H. IMAGING ANALYSIS

While conducting imaging experiments, data was acquired using a custom-made control system. The obtained images were gathered and shown by using a custom program in Visual Studio (Microsoft). The control board converted analog signals from the image sensor to 14-bit digital signals.

The fluorescence difference (ΔF) was defined as the difference between F and F_0. F_0 was the average fluorescence intensity within the region of interest (ROI, 9 × 9 pixels, 67.5 μm × 67.5 μm) in the reference image collected at time zero (t = 0) (i.e., immediately before nicotine administration). F was the average value of the same ROI after nicotine administration. The fluorescence ratio was calculated as $\Delta F/F_0$ (Eq.1). Fig. 5(D) and Fig. 6(D) indicated $\Delta F/F_0$ by using pseudo color. The values in Fig. 5(D) and Fig. 6(D) indicated the fluorescence ratio (%), $\Delta F/F_0$, of the ROI.

$$\frac{\Delta F}{F_0} = \frac{F - F_0}{F_0} \qquad \text{(Eq.1)}$$

The fluorescence intensity is related to the activity of DA neurons in the VTA, and not directly related with concentration of DA release in the NAc and the PFC. We have evaluated fluorescence detection performance by using fluorescein-4-isothiocyanate (FITC-I) solutions by dissolving FITC-I in a standard turbidity solution with our previous device as detailed in [19].

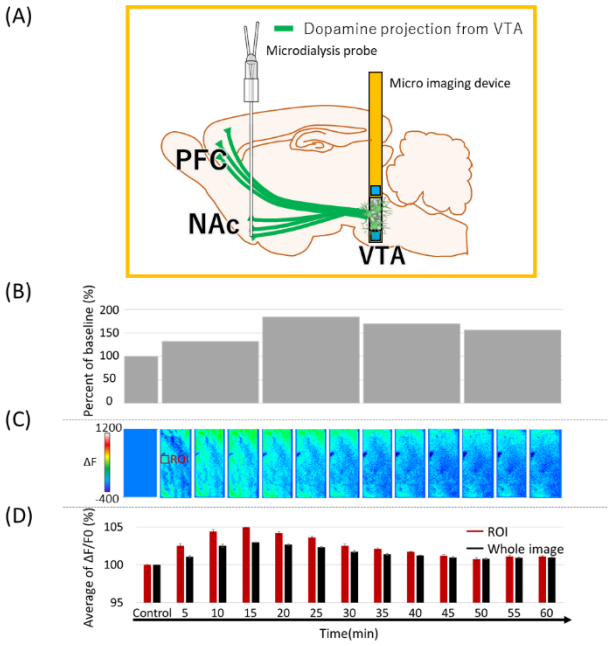

FIGURE 5. DA release measurement in the PFC and GCaMP fluorescence imaging in the VTA associated with 0.25 mg/kg nicotine administration. Nicotine was introduced by IP injection. (A) Schematic of the probe in the PFC and the imaging device was in the VTA. (B) Percentage DA release amount compared with baseline. Control (baseline) was estimated by DA release amount measured before nicotine administration. (C) Representative time-lapse fluorescence images of every 5 minutes of the mouse's VTA. (D) The fluorescence ratio of the ROI (9 × 9 pixels, 67.5 μm ×67.5 μm) and whole images, ΔF/ F0 (%), increased following nicotine administration.

I. IMPLANTATION SITE CONFIRMATION

In order to confirm the position of the device and the appearance of GCaMP fluorescence, we obtained brain slices after the experiments using a LinearSlicer PRO7 (DOSAKA EM CO.,LTD, Japan). The slices were fixed overnight using 4% paraformaldehyde (PFA, FUJIFILM Wako Pure Chemical Co.) before image acquisition.

J. STATISTICAL ANALYSIS

Repeated measures analysis of variance (ANOVA) was used to identify statistically significant differences in fluorescence ratios at each time point. A p-value < 0.05 was considered significant. Data is represented as mean ± standard error.

III. RESULTS

A. GCaMP6 IMAGING OF DA NEURON AND MEASUREMENT OF DA RELEASE WITH NICOTINE INTAKE

The relationship between DA neuron activity in the VTA and DA release in the PFC or the NAc has been investigated by several groups using several methods including electrophysiology, imaging, and microdialysis [1], [2], [5], [22]. To investigate the DA network system at the neural level, we monitored DA neuron activity in the VTA using the implantable imaging device and simultaneously measured DA release in the PFC or the NAc by the microdialysis system. We focused

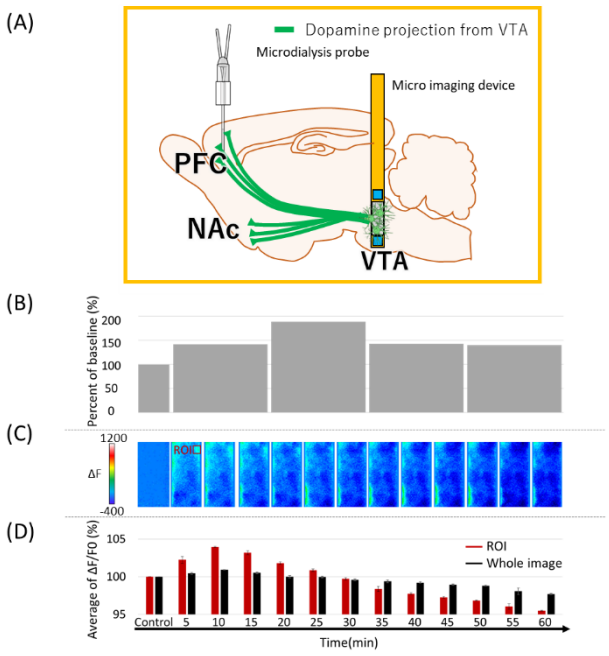

FIGURE 6. DA release measurement in the NAc and GCaMP fluorescence imaging in the VTA associated with 0.25 mg/kg nicotine administration. Nicotine was introduced by IP injection. (A) Schematic of the probe and the imaging device position. The probe was in the NAc and the imaging device was in the VTA. (B) Percentage DA release amount compared with baseline. Control (baseline) was estimated by DA release amount measured before nicotine administration. (C) Representative time-lapse fluorescence images of every 5 minutes of the mouse's VTA. (D) The fluorescence ratio of the ROI (9 × 9 pixels, 67.5 μm ×67.5 μm) and whole images, ΔF/ F0 (%), increased following nicotine administration.

on the interaction of the fluorescence difference (ΔF) and the amount of DA release (% Baseline) to the amount of nicotine intake.

For the first experiment, we monitored the changes in the fluorescence intensity in the VTA and measured the amount of DA release in the PFC over 60 minutes as shown in Fig 5(A). We show fluorescence intensity in the VTA and DA release in the PFC increased after nicotine administration. In the microdialysis experiment, we measured DA release in the PFC to determine baseline DA (i.e., before nicotine administration). After the animal became stable, we injected nicotine IP to the mouse and gathered microdialysis samples every 15 minutes. Fig. 5(B) shows the percentage of DA release compared to baseline. Release of DA in the PFC increased over the first 30 minutes and slightly decreased after 30 minutes and continued to 60 minutes. These results are similar to previous studies [23].

We estimated the average fluorescence ratio (ΔF/F0 (%)) over 1 minute in a ROI to represent parts of whole images areas shown in Fig. 5(C, D). The ROI consisted of 9 × 9 pixels (67.5 μm × 67.5 μm) and was selected due to high fluorescent intensity area. Fig. 5(C, D) representative images collected every 5 minutes and the ΔF/F0(%) of the ROI. ΔF/F0 was also increased after the nicotine administration during the first 15 minutes and gradually decreased after

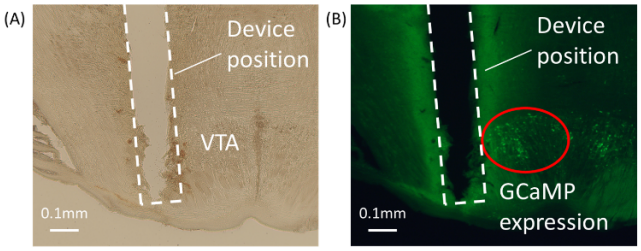

FIGURE 7. Representative images of a mouse coronal brain slice that was prepared after the imaging and the microdialysis experiments. (A) Bright field image of the VTA. The imaging device position is framed by while dot line. (B) Fluorescence image of a brain slice. The GCaMP expression is circled with red solid line and the location of our device is marked as a white dot line. Scale bar is 0.1 mm.

15 minutes, consistent with a previous study which used 0.30 mg/kg nicotine to excite DA release [23].

We next monitored the changes in the fluorescence intensity within the VTA and measured the amount of DA release in the NAc from a different animal over 60 minutes as shown in Fig. 6(A). DA release in the PFC was quantified at baseline and after the acute nicotine dose experiment. Samples were gathered over the same conditions as described above and are shown in the Fig. 6(B).

ΔF/F0 (%) was also measured and estimated every 1 minute in a ROI to represent parts of whole images areas shown in Fig. 6(C, D). The ΔF/F0 increased during the first 10 minutes and slightly decreased afterwards. These findings are consistent with a previous study which used 0.30 mg/kg nicotine to excite DA release [23].

These results provide valuable evidence that GCaMP fluorescence imaging and microdialysis measurements can be conducted simultaneously using our novel implantable imaging system and a microdialysis system.

B. THE POSITION OF IMPLANTED DEVICE AND GCaMP PRESENCE IN THE VTA

GCaMP expressions were observed in VTA using our implantable microimaging device as illustrated in Fig. 5(C) and Fig. 6(C). To verify the fluorescence reaction measured was produced by GCaMP expression in the VTA, we confirmed the position of the device and the presence of GCaMP. Fig. 7(A) and (B) show the bright field and fluorescence images of a coronal brain slice from a GCaMP mouse. The photographs show a small scar made by the implantable imaging device, and GCaMP expressions is denoted by red circle. Combined, these results suggest that the device was implanted within the VTA.

IV. DISCUSSION

Nicotine is deeply related with DA neural activities in the VTA and increased DA release in the PFC and the NAc. This is a complex neural network system involved in drug reward and addiction [24]–[29]. Additionally, the neural network system has not been fully understood due to difficulty of monitoring brain activities in several areas simultaneously.

In this study, we investigated DA neurons in the VTA and DA release in the PFC or the NAc in response to nicotine exposure. Our goal was to monitor the DA neural network system by combining an implantable microimaging device and a traditional microdialysis system. We used transgenic GCaMP mice to observe neural activities via fluorescence and our implantable microimaging device and recorded the fluorescence reaction associated with nicotine intake. Fluorescence intensity within the VTA increased during the first 10 minutes following exposure and gradually decreased after 15 minutes following nicotine exposure.

According to these results, maximum ΔF/F0 was 5.1% when 0.25 mg/kg of nicotine was administered. However, this result was lower than what has been reported in the literature [13]. Wei *et al.*, showed that at the high dose of nicotine the production of GCaMP increased approximately 55% [13]. The lower results in our study could be due to the higher background intensity [13] and type of transgenic mice. In fluorescence microscopy, ΔF is calculated by considering only the fluorescence ratio intensities since the background value is close to 0 (Eq.1). However, the background value (B) of the implantable microimaging device cannot be considered 0 because of the excitation light leakage. Then, $\Delta F/F_0$ for implantable microimaging device can be calculated using Eq. 2(A) and (B). F' and F_0 indicated unmeasured fluorescence intensity by the implantable microimaging device. Therefore, it is possible that $\Delta F/F_0$ of the implantable microimaging device resulted in a decreased intensity rate in GCaMP compared to the results from Wei *et al.* [13].

$$F = F' + \mathrm{B}, \quad F_0 = F_0' + \mathrm{B} \qquad \text{(Eq. 2(A))}$$

$$\frac{\Delta F}{F_0} = \frac{(F' + B) - (F_0' + B)}{F_0' + B} = \frac{F' - F_0'}{F_0' + B} \qquad \text{(Eq. 2(B))}$$

Additionally, we used GCaMP transgenic mice to observe DA neural activities, however, these animals were not specific transgenic mice for targeting DA neurons. GCaMP expression can be lower than specific models such as the animals used in Wei *et al.* Due to the transgenic animal model, both DA neurons and GABA neurons had GCaMP. Therefore, although we believe the fluorescence imaging data included the response from GABA neurons, previous studies have shown that nicotine acts predominantly on DA neurons compared with GABA neurons [29]. To address this problem, future studies will introduce Dopamine Transporter (DAT) Cre animals. The DAT-Cre model expresses Cre-recombinase under the control of the endogenous DA transporter promoter, enabling specific expression in DA neurons. Furthermore, we will investigate only DA neural activity by combining GCaMP fluorescence and DAT-Cre animals with several nicotine doses.

We used a traditional microdialysis system to measure DA release associated with nicotine in the PFC and the NAc. DA release increased after nicotine administration in the both areas. DA release intake in both areas gradually increased and reached a maximum during the first 30 minutes following nicotine. 30 minutes after nicotine intake, DA release began to decrease, but was still higher than baseline. These results were similar to previous studies using microdialysis experiments in the PFC and the NAc following nicotine administration. In Fig. 5(B), the highest DA release occurred just after highest GCaMP fluorescence reaction. This result could be in part due to nicotine intake which excited DA neurons in the VTA, which subsequently induced DA release in the PFC. DA release began to decrease shortly after the fluorescence reactions began to diminish as well. Fluorescence intensity of the ROI decreased much faster in the NAc than the PFC. However, DA release also correlated to fluorescence reactions in the VTA.

V. SUMMARY

In this study, we demonstrated that GCaMP fluorescence in the VTA and DA release in the PFC and NAc is associated with nicotine intake can be measured simultaneously by a novel platform that combines an implantable microimaging device and a microdialysis probe. We used GCaMP transgenic mice and a dedicated fluorescence imaging system with a traditional microdialysis system to monitor neural activities within the VTA, PFC and NAc. GCaMP fluorescence and DA release reactions related to nicotine intake were measured simultaneously. The methods introduced in this study will be used to investigate the neural network including the VTA, PFC and NAc in future studies to further quantify DA dynamics.

ACKNOWLEDGMENT

The authors would like to thank to the VLSI Design and Education Center (VDEC), the University of Tokyo and the Cadence Corporation and Mentor Graphics Corporation for their kind support. The authors are also grateful to Dr. Charlotte Mae K. Waits for her assistance editing this manuscript. *(Yoshinori Sunaga and Yasumi Ohta are co-first authors.)*

REFERENCES

[1] S. Lohani *et al.*, "Burst activation of dopamine neurons produces prolonged post-burst availability of actively released dopamine," *Neuropsychopharmacology*, vol. 43, no. 10, pp. 2083–2092, 2018, doi: 10.1038/s41386-018-0088-7.

[2] I. T. Ellwood, T. Patel, V. Wadia, A. T. Lee, A. T. Liptak, K. J. Bender, and V. S. Sohal, "Tonic or phasic stimulation of dopaminergic projections to prefrontal cortex causes mice to maintain or deviate from previously learned behavioral strategies," *J. Neurosci.*, vol. 37, no. 35, pp. 8315–8329, Aug. 2017.

[3] M. Pignatelli and A. Bonci, "Role of dopamine neurons in reward and aversion: A synaptic plasticity perspective," *Neuron*, vol. 86, no. 5, pp. 1145–1157, Jun. 2015.

[4] R. Narendran, H. P. Jedema, B. J. Lopresti, N. S. Mason, K. Gurnsey, J. Ruszkiewicz, C. M. Chen, L. Deuitch, W. G. Frankle, and C. W. Bradberry, "Imaging dopamine transmission in the frontal cortex: A simultaneous microdialysis and [11 C] FLB 457 PET study," *Mol. Psychiatry*, vol. 19, no. 3, pp. 302–310, 2014.

[5] T. Patriarchi, J. R. Cho, K. Merten, M. W. Howe, A. Marley, W.-H. Xiong, R. W. Folk, G. J. Broussard, R. Liang, M. J. Jang, H. Zhong, D. Dombeck, M. von Zastrow, A. Nimmerjahn, V. Gradinaru, J. T. Williams, and L. Tian, "Ultrafast neuronal imaging of dopamine dynamics with designed genetically encoded sensors," *Science*, vol. 360, no. 6396, pp. 1–15, Jun. 2018.

[6] J. H. Jennings, R. L. Ung, S. L. Resendez, A. M. Stamatakis, J. G. Taylor, J. Huang, K. Veleta, P. A. Kantak, M. Aita, K. Shilling-Scrivo, C. Ramakrishnan, K. Deisseroth, S. Otte, and G. D. Stuber, "Visualizing hypothalamic network dynamics for appetitive and consummatory behaviors," *Cell*, vol. 160, no. 3, pp. 516–527, Jan. 2015.
[7] K. Murari, R. Etienne-Cummings, G. Cauwenberghs, and N. Thakor, "An integrated imaging microscope for untethered cortical imaging in freely-moving animals," in *Proc. Annu. Int. Conf. IEEE Eng. Med. Biol.*, vol. 10, Aug. 2010, pp. 5795–5798.
[8] J. H. Park, J. Platisa, J. V. Verhagen, S. H. Gautam, A. Osman, D. Kim, V. A. Pieribone, and E. Culurciello, "Head-mountable high speed camera for optical neural recording," *J. Neurosci. Methods*, vol. 201, no. 2, pp. 290–295, Oct. 2011.
[9] K. K. Ghosh, L. D. Burns, E. D. Cocker, A. Nimmerjahn, Y. Ziv, A. E. Gamal, and M. J. Schnitzer, "Miniaturized integration of a fluorescence microscope," *Nature Methods*, vol. 8, no. 10, pp. 871–878, Oct. 2011.
[10] W. Zong, R. Wu, M. Li, Y. Hu, Y. Li, J. Li, H. Rong, H. Wu, Y. Xu, Y. Lu, H. Jia, M. Fan, Z. Zhou, Y. Zhang, A. Wang, L. Chen, and H. Cheng, "Fast high-resolution miniature two-photon microscopy for brain imaging in freely behaving mice," *Nature Methods*, vol. 14, no. 7, pp. 713–719, Jul. 2017.
[11] Y.-J. Luo, Y.-D. Li, L. Wang, S.-R. Yang, X.-S. Yuan, J. Wang, Y. Cherasse, M. Lazarus, J.-F. Chen, W.-M. Qu, and Z.-L. Huang, "Nucleus accumbens controls wakefulness by a subpopulation of neurons expressing dopamine d1 receptors," *Nature Commun.*, vol. 9, no. 1, pp. 1–7, Dec. 2018.
[12] I. Ferezou, S. Bolea, and C. C. H. Petersen, "Visualizing the cortical representation of whisker touch: Voltage-sensitive dye imaging in freely moving mice," *Neuron*, vol. 50, no. 4, pp. 617–629, May 2006.
[13] C. Wei, X. Han, D. Weng, Q. Feng, X. Qi, J. Li, and M. Luo, "Response dynamics of midbrain dopamine neurons and serotonin neurons to heroin, nicotine, cocaine, and MDMA," *Cell Discovery*, vol. 4, no. 1, pp. 1–16, Dec. 2018.
[14] S. L. Resendez, J. H. Jennings, R. L. Ung, V. M. K. Namboodiri, Z. C. Zhou, J. M. Otis, H. Nomura, J. A. McHenry, O. Kosyk, and G. D. Stuber, "Visualization of cortical, subcortical and deep brain neural circuit dynamics during naturalistic mammalian behavior with head-mounted microscopes and chronically implanted lenses," *Nature Protocols*, vol. 11, no. 3, pp. 566–597, Mar. 2016.
[15] J. Ohta, Y. Ohta, H. Takehara, T. Noda, K. Sasagawa, T. Tokuda, M. Haruta, T. Kobayashi, Y. M. Akay, and M. Akay, "Implantable microimaging device for observing brain activities of rodents," *Proc. IEEE*, vol. 105, no. 1, pp. 158–166, Jan. 2017.
[16] Y. Sunaga, Y. Ohta, Y. M. Akay, J. Ohta, and M. Akay, "Monitoring neural activities in the VTA in response to nicotine intake using a novel implantable microimaging device," *IEEE Access*, vol. 8, pp. 68013–68020, 2020.
[17] H. Takehara, Y. Ohta, M. Motoyama, M. Haruta, M. Nagasaki, H. Takehara, T. Noda, K. Sasagawa, T. Tokuda, and J. Ohta, "Intravital fluorescence imaging of mouse brain using implantable semiconductor devices and epi-illumination of biological tissue," *Biomed. Opt. Exp.*, vol. 6, no. 5, p. 1553, 2015.
[18] A. Tagawa, A. Higuchi, T. Sugiyama, K. Sasagawa, T. Tokuda, H. Tamura, Y. Hatanaka, Y. Ishikawa, S. Shiosaka, and J. Ohta, "Development of complementary metal oxide semiconductor imaging devices for detecting green fluorescent protein in the deep brain of a freely moving mouse," *Jpn. J. Appl. Phys.*, vol. 48, no. 4, Apr. 2009, Art. no. 04C195.
[19] Y. Sunaga, H. Yamaura, M. Haruta, T. Yamaguchi, M. Motoyama, Y. Ohta, H. Takehara, T. Noda, K. Sasagawa, T. Tokuda, Y. Yoshimura, and J. Ohta, "Implantable imaging device for brain functional imaging system using flavoprotein fluorescence," *Jpn. J. Appl. Phys.*, vol. 55, no. 3S2, Mar. 2016, Art. no. 03DF02.
[20] M. Haruta, Y. Kurauchi, M. Ohsawa, C. Inami, R. Tanaka, K. Sugie, A. Kimura, Y. Ohta, T. Noda, K. Sasagawa, T. Tokuda, H. Katsuki, and J. Ohta, "Chronic brain blood-flow imaging device for a behavioral experiment using mice," *Biomed. Opt. Exp.*, vol. 10, no. 4, p. 1557, 2019.
[21] M. Haruta, Y. Sunaga, T. Yamaguchi, H. Takehara, T. Noda, K. Sasagawa, T. Tokuda, and J. Ohta, "Intrinsic signal imaging of brain function using a small implantable CMOS imaging device," *Jpn. J. Appl. Phys.*, vol. 54, no. 4, Apr. 2015, Art. no. 04DL10.
[22] S. Lohani, A. K. Martig, K. Deisseroth, I. B. Witten, and B. Moghaddam, "Dopamine modulation of prefrontal cortex activity is manifold and operates at multiple temporal and spatial scales," *Cell Rep.*, vol. 27, no. 1, pp. 99–114.e6, 2019.
[23] S. Rossi, S. Singer, E. Shearman, H. Sershen, and A. Lajtha, "The effects of cholinergic and dopaminergic antagonists on nicotine-induced cerebral neurotransmitter changes," *Neurochem. Res.*, vol. 30, no. 4, pp. 541–558, Apr. 2005.
[24] D. Zhang, M. Gao, D. Xu, W.-X. Shi, B. S. Gutkin, S. C. Steffensen, R. J. Lukas, and J. Wu, "Impact of prefrontal cortex in nicotine-induced excitation of ventral tegmental area dopamine neurons in anesthetized rats," *J. Neurosci.*, vol. 32, no. 36, pp. 12366–12375, Sep. 2012.
[25] H. Chen, S. L. Parker, S. G. Matta, and B. M. Sharp, "Gestational nicotine exposure reduces nicotinic cholinergic receptor (nAChR) expression in dopaminergic brain regions of adolescent rats," *Eur. J. Neurosci.*, vol. 22, no. 2, pp. 380–388, Jul. 2005.
[26] A. B. Gold, A. B. Keller, and D. C. Perry, "Prenatal exposure of rats to nicotine causes persistent alterations of nicotinic cholinergic receptors," *Brain Res.*, vol. 1250, pp. 88–100, Jan. 2009.
[27] A. Fallis, "Two projection systems from the ventral midbrain to the nucleus accumbens-olfactory tubercle complex," *J. Chem. Inf. Model.*, vol. 53, no. 9, pp. 1689–1699, 2013.
[28] D. Zhang, A. Dragomir, Y. M. Akay, and M. Akay, "Nicotine exposure increases the complexity of dopamine neurons in the parainterfascicular nucleus (PIF) sub-region of VTA," *J. Neuroeng. Rehabil.*, vol. 11, no. 1, pp. 1–6, 2014.
[29] R. F. Keller, T. Kazemi, A. Dragomir, Y. M. Akay, and M. Akay, "Comparison between dopaminergic and non-dopaminergic neurons in the VTA following chronic nicotine exposure during pregnancy," *Sci. Rep.*, vol. 9, no. 1, pp. 1–13, Dec. 2019.

YOSHINORI SUNAGA received the B.E. degree from Chiba University, Japan, in 2012, the M.E. and Ph.D. degrees from the Graduate School of Materials Science, Nara Institute of Science and Technology (NAIST), Japan, in 2014 and 2017, respectively. In 2017, he joined NAIST as a Postdoctoral Fellow and started collaboration research between NAIST and the University of Houston. In 2019, he joined the University of Houston as a Postdoctoral Fellow. He is interested in development of novel devices for observing and accessing brain activity of animals to reveal new brain mechanism.

YASUMI OHTA received the Ph.D. degree in biophysics science from Kyoto University, Kyoto, Japan, in 2011. In 2011, she joined the Nara Institute of Science and Technology, Nara, Japan as a Postdoctoral Fellow. Her research interests include implantable bioimaging CMOS sensors and neuroscience

TAKAAKI E MURAKAMI received the B.E. degree in electrical and electronic engineering from Kindai University, Osaka, Japan, in 2020. He is currently pursuing the M.E. degree with the Nara Institute of Science and Technology (NAIST), Nara, Japan.

YASEMIN M. AKAY (Senior Member, IEEE) received the B.S. degree in pharmaceutical sciences from Hacettepe University, Ankara, Turkey, in 1980, and the M.S. and Ph.D. degrees in biomedical engineering from Rutgers University, Piscataway, NJ, USA, in 1991 and 1998, respectively. She was a Postdoctoral Fellow with the Physiology and Pharmacology Departments, Dartmouth Medical School and with the Department of Physiology and Biophysics, Boston University, School of Medicine. She is currently an Instructional and a Research Assistant Professor with the Department of Biomedical Engineering, Cullen College of Engineering, University of Houston, Houston, TX, USA. Her current research interests include molecular neuroengineering, neural growth, and neurodegeneration. She is an Associate Editor for the IEEE Open Journal of Engineering in Medicine and Biology of the IEEE Engineering in Medicine and Biology Society and the *IJMS*.

JUN OHTA (Fellow, IEEE) received the B.E., M.E., and Dr.Eng. degrees in applied physics from The University of Tokyo, Japan, in 1981, 1983, and 1992, respectively. In 1983, he joined Mitsubishi Electric Corporation, Hyogo, Japan. From 1992 to 1993, he was a Visiting Scientist with the Optoelectronics Computing Systems Center, University of Colorado Boulder. In 1998, he joined the Graduate School of Materials Science, Nara Institute of Science and Technology (NAIST), Nara, Japan as an Associate Professor. He was appointed as a Professor, in 2004. His current research interests include smart CMOS image sensors for biomedical applications and retinal prosthetic devices. He is a Fellow of the Japan Society of Applied Physics and the Institute of Image, Information, and Television Engineers. He serves as an Associate Editor of IEEE Transactions on Biomedical Circuits and Systems, and an Editorial Board of *Journal of Engineering*, IET.

METIN AKAY (Fellow, IEEE) received the B.S. and M.S. degrees in electrical engineering from Bogazici University, Istanbul, Turkey, in 1981 and 1984, respectively, and the Ph.D. degree from Rutgers University, Piscataway, NJ, USA, in 1990. He is currently the Founding Chair of the Department of Biomedical Engineering, University of Houston. His current research interests include investigation of nicotine and alcohol addiction at the molecular, cellular and system levels during maturation and the development of brain chip for precision medicine. He is also the President of the IEEE EMBS. He was the Founding Chair of the Annual International Summer School on BIO-X sponsored by the National Science Foundation (NSF) and technically co-sponsored by the IEEE EMBS, of the Satellite Conference on Emerging Technologies in Biomedical Engineering. He was the Founding Chair of the International IEEE Conference on Neural Engineering, in 2003.